Available online at www.sciencedirect.com

SciVerse ScienceDirect

Ceramics International 38 (2012) 3791–3800

CERAMICS INTERNATIONAL

www.elsevier.com/locate/ceramint

Effect of Al_4SiC_4 on the Al_2O_3–SiC–SiO_2–C refractory castables performance

A.P. Luz [a,*], M.M. Miglioli [a], T.M. Souza [a], S. Hashimoto [b], S. Zhang [c], V.C. Pandolfelli [a]

[a] Federal University of São Carlos, Materials Engineering Department, Rod. Washington Luiz, km 235, São Carlos, SP 13565-905, Brazil
[b] Department of Environmental and Materials Engineering, Nagoya Institute of Technology, Nagoya 466-8555, Japan
[c] University of Sheffield, Materials Science and Engineering Department, Sheffield S1 3JD, United Kingdom

Received 18 December 2011; received in revised form 9 January 2012; accepted 10 January 2012
Available online 18 January 2012

Abstract

Carbon-containing refractories are widely used in the steelmaking process due to their outstanding properties and, in order to improve their oxidation resistance, the so-called antioxidants have often been used. Al_4SiC_4 is pointed out as a novel additive that presents suitable properties such as Al, but without its drawbacks. Therefore, the effect of Al_4SiC_4 addition to Al_2O_3–SiC–SiO_2–C castables designed for lining blast furnace troughs was investigated in this work. Apparent porosity, oxidation, thermogravimetric, X-ray diffraction, hot elastic modulus tests and thermodynamic calculations were carried out in order to better understand the antioxidant effects and reaction mechanisms. Additionally, the collected results were compared with those from the compositions containing other commonly used antioxidants (Si, B_4C and sodium borosilicate glass). The performance of the novel additive proved to be limited as most of the carbon source used reacted earlier than the Al_4SiC_4 action. As a consequence, intense carbon oxidation, along with the thermal expansion mismatch among the phases during the cooling step, intensified the deterioration of the evaluated refractory material.

Keywords: D. Carbon; Al_4SiC_4; Antioxidant; Oxidation; Refractory castables

---

1. Introduction

High-carbon-containing refractory castables are widely used in blast furnace troughs due to their high refractoriness, thermal shock resistance and low wettability by molten slag [1–3]. Carbon presents many of the desired properties for the refractories, however the main drawback is its high susceptibility to oxidation. In recent years, numerous studies have been carried out to investigate the effect of metallic and non-metallic antioxidant additions on the oxidation resistance and mechanical properties of carbon-containing refractory castables [4–7]. Moreover, the use of both, single or multiple antioxidant sources has been widely discussed [8–11].

Aluminum (Al) is one of the most extensively used antioxidants in refractory compositions. However, its by-product can be Al_4C_3, which may lead to disintegration of castables due to the poor hydration resistance of this phase [12,13]. In addition, in the presence of cement, the Al–H_2O reaction during the castables mixing step takes place much earlier and faster, negatively affecting the performance of this additive to further decrease the carbon oxidation [14]. In order to overcome such effects, some efforts have been made to develop alternative antioxidants presenting suitable properties but with less drawbacks. In this sense, aluminum silicon carbide (Al_4SiC_4) is a promising material due to its low density (3.03 g cm^{-3}), high melting point (>2000 °C) and good oxidation and hydration resistances. Its action takes place above 750 °C leading to the formation of a protective coating comprised by Al_2O_3 and mullite (Eqs. (1)–(3)) on the refractory particles, which fills in the pores, preventing further carbon oxidation [15].

$$Al_4SiC_4 + 6O_2 \rightarrow 2Al_2O_3 + SiC + 3CO_2 \quad (1)$$

$$SiC + 2O_2 \rightarrow SiO_2 + CO_2 \quad (2)$$

$$3Al_2O_3 + 2SiO_2 \rightarrow 2Al_6Si_2O_{13} \quad (3)$$

Various methods for synthesizing Al_4SiC_4 have been investigated by using metals (Al and Si), carbides (Al_4C_3

---

* Corresponding author. Tel.: +55 16 33518253; fax: +55 16 33615404.
E-mail address: anapaula.light@gmail.com (A.P. Luz).

0272-8842/$36.00 © 2012 Elsevier Ltd and Techna Group S.r.l. All rights reserved.
doi:10.1016/j.ceramint.2012.01.027

and SiC) or oxides (Al_2O_3, SiO_2 and kaolin) as starting raw materials [12,13,15–17]. Barczak [18] prepared this complex carbide powder using a 4:1 molar ratio mixture of Al and Si with excess of carbon in a sealed container at 1620 °C for 10 min. Other authors [15,16] produced this compound by heating a mixture of Al, Si and C in argon atmosphere at 1700 °C. By mixing the starting materials (Al, Si and C) with $N(CH_2CH_2OH)$, Yamamoto et al. [19] managed to reduce the synthesis temperature to 1450 °C. Hot-pressing at 1750–1980 °C or sintering at 1600 °C using fine SiC and Al_4C_3 powders in argon atmosphere were also considered for this purpose [20,21]. In addition, Al_4SiC_4 was synthesized by heating a mixture of Al, Si, C and 3 wt% of Al_2O_3, Al, kaolin and C or Al_2O_3, SiO_2 and C at 1700 °C [13,15,16]. Various parameters can affect the efficiency of these methods, such as the mixture/contact of the raw materials (powder or pressed compact), heating temperature, heating time, chosen atmosphere and the component ratios.

Nevertheless, despite the various improvements in the Al_4SiC_4 synthesis procedures, to the best of our knowledge not much research has focused on evaluating this antioxidant performance in refractory compositions (mainly, MgO–C and Al_2O_3–C bricks) [12,22,23]. Therefore, there is a lack of studies concerning the analysis of this aluminum silicon carbide behavior in cement-bonded castables.

Considering these aspects, this work aims to evaluate the Al_4SiC_4 performance in high carbon-containing castable compositions (Al_2O_3–SiC–SiO_2–C) designed for lining blast furnace troughs. Furthermore, a comparison among the collected results and the ones attained for other antioxidant additives commonly used in steelmaking refractory materials (Si, B_4C and sodium borosilicate glass) was also carried out. Apparent porosity, oxidation resistance, thermogravimetry, X-ray diffraction, hot elastic modulus tests and thermodynamic calculations were performed in order to better understand the phase transformations and the antioxidant effect in the castables properties.

2. Experimental

2.1. Al_4SiC_4 synthesis procedure

Aluminum (average particle size: 3 μm, purity: 99.9%), carbon (average particle size: 5 μm, purity: 99.9%) and SiC (average particle size: 2–3 μm, purity: 99%) powders by Kojundo Chemical Lab. Co. Ltd., Japan, were used as the starting raw materials. Al and C were firstly mixed in a 4:3 molar ratio, uniaxially pressed at 13 MPa, and the attained pellet was thermally treated in argon for 2 h at 1400 °C to give rise to the Al_4C_3 phase. The prepared Al_4C_3 was then mixed with SiC in an equimolar ratio and subjected to the same pressing procedure. After firing for 2 h at 1700 °C in a vacuum, the pellet consisting of pure Al_4SiC_4 was then crushed and ground to a material with an average particle size below 10 μm (Fig. 1).

2.2. Design, processing and evaluation of the carbon-containing castables

Four self-flow Al_2O_3–SiC–SiO_2–C refractory castable compositions with ultralow cement content were designed (Table 1), according to the Alfred packing model ($q = 0.21$) [24]. An antioxidant-free castable was prepared to be used as a reference material. Additionally, Al_4SiC_4, silicon powder (Si, Elkem Refractories, Norway, average particle size < 75 μm), boron carbide (B_4C, China Brasilis, China, average particle size = 32 μm) and sodium borosilicate glass (BS, Ferro Enamel, Brazil, BS – average particle size = 20 μm) were used as antioxidants in the other formulations listed in Table 1. According to previous studies [8,9], the addition of an antioxidant blend ($Si + B_4C + BS$) can protect the carbon sources in a broader temperature range, resulting in some beneficial effects, such as the increase in hot mechanical strength due to the in situ formation of SiC and mullite [9]. Therefore, refractory castables comprising this antioxidant blend (5SBC) or only boron carbide (2B) were also prepared and compared to the one containing Al_4SiC_4 (2A).

The dispersion of the castables was carried out using an electrosteric dispersant (0.2 wt%, Darvan-7S, R.T. Vanderbilt, Norwalk, Conn.) and a non-ionic surfactant (HLB = 8, 4.0 mg/m^2) as wetting agent for the carbon sources [25,26]. Before casting, the compositions were dry-homogenized for 1 min and mixed in a rheometer developed for refractory castables [27] for an additional 5 min, by adding 6.3 wt% of water to the antioxidant blend-containing castable and 5.4 wt% to the other ones.

Cylindrical samples ($d = 40$ mm and $h = 40$ mm) were prepared and cured at 50 °C for 12 h (relative humidity ~ 80%),

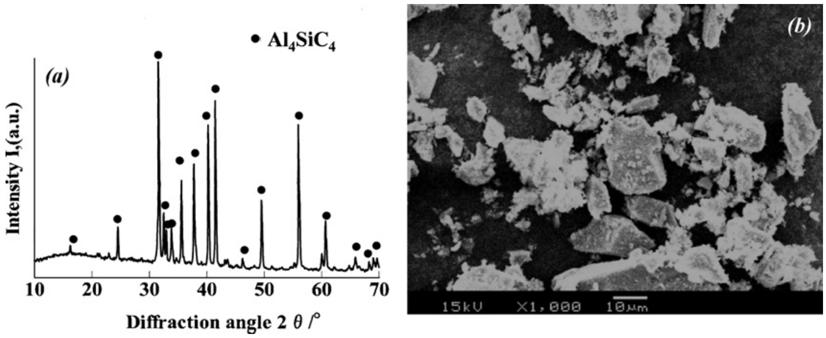

Fig. 1. (a) XRD pattern and (b) typical SEM image of the synthesized Al_4SiC_4 powder.

Table 1
High-carbon-containing castable compositions evaluated in this work.

Raw materials (wt%)	R	2A	2B	5SBC
Tabular alumina (6–0.2 mm)[a]	53	47	47	44
Silicon carbide (6–0.2 mm)[b]	20	20	20	20
Calcined alumina (CL370C)[a]	14	18	18	16
Calcium aluminate cement (Secar71)[a]	2	2	2	2
Silica fume (971-U)[c]	1	1	1	1
Al_4SiC_4 (<50 μm)	–	2	–	–
Silicon powder (Silgrain)[c]	–	–	–	5
Sodium borosilicate glass[d]	–	–	–	1
Boron carbide[e]	–	–	2	1
Coke[f]	2	2	2	2
Pitch[f]	5	5	5	5
Carbon black[f]	3	3	3	3
Water content (%)	5.4	5.4	5.4	6.3
Free-flow (%)	58 ± 4	53 ± 3	53 ± 3	57 ± 2

[a] Almatis, EUA.
[b] Treibacher, Brazil.
[c] Elkem Refractories, Norway.
[d] Ferro Enamel, Brazil.
[e] China Brasilis, China.
[f] Unimetal and Nacional de Grafite, Brazil.

80%), dried at 110 °C for 24 h, followed by firing at 600, 900, 1200 and 1500 °C for 5 h in an electrical furnace (Lindberg Blue, Lindberg Corporation, USA) in oxidizing atmosphere (oxygen partial pressure = 0.21 atm, heating rate = 2 °C min^{-1}) for the apparent porosity and oxidation resistance tests. The apparent porosity after drying and firing was measured by the Archimedes method (ASTM C380-00), using kerosene as the immersion liquid. Furthermore, after the thermal treatments, the decarbonized areas of the samples were measured (Image J 1.42q software, Wayne Rasband, National Institutes of Health, USA) to attain a quantitative analysis of the carbon oxidation evolution.

The mass changes of each carbon sources (coke, pitch and carbon black), Al_4SiC_4 and a mixture of Al_4SiC_4 and pitch (in a weight ratio of 1:1) were recorded as a function of temperature (30 up to 1400 °C) by thermogravimetric experiments [NETZSCH STA 449 equipment, using a heating rate of 5 °C min^{-1} with a synthetic air (80% N_2–20% O_2) flow of 50 cm^3/min and α-Al_2O_3 as a correction standard]. The aim of these tests was to detect the beginning of the carbon oxidation and the Al_4SiC_4 reactions with O_2 and CO.

For the hot elastic modulus tests, some prismatic samples (150 mm × 25 mm × 25 mm) attained after curing and drying steps were evaluated according to ASTM C 1198-91 using the resonance bar technique (Scanelastic equipment, ATCP, Brazil), which is based on sample excitation and the detection of the correspondent vibration spectrum using piezoelectric transducers [28]. For the fundamental flexural frequency of a rectangular bar, the Young's modulus is given by:

$$E = 0.9465\frac{m f_f^2}{b} \times \frac{L^3}{t^3} \times T_1 \qquad (4)$$

where E is the Young's modulus (Pa), m is the mass (g), b is the width (mm), L is the length (mm), t is the thickness (mm), f_f is the fundamental resonance frequency of the bar in flexure (Hz), and T_1 is the correction factor for fundamental flexural mode to account for finite thickness of the bar, Poisson's ratio and others. The measurements were carried out in the 30–1200 °C range in air ($pO_2 = 0.21$ atm) with a heating rate of 2 °C min^{-1}, in order to follow the antioxidant transformations and carbon oxidation effects on the castable performance.

The oxidized castables were also ground (dp < 45 μm) in a tungsten carbide mill (AMEF, model AMP1-M, Brazil) and analyzed using the X-ray diffraction technique (Bruker equipment, model D8 Focus, Germany) and EVA software. The Rietveld method (Topas 4.2 software, Bruker) was used to quantitatively analyze the XRD profiles.

Thermodynamic simulations were carried out using FactSage^{TM} [version 6.2, Thermfact/CRCT (Montreal) and GTT-Technologies (Aachen)] for oxidizing ($pO_2 = 0.21$ atm) atmosphere in order to predict the castables' phase composition as a function of the temperature (600–1500 °C). The databases Fact53, SGTE and FToxid were used and the Equilib and Phase Diagram modules selected for the chosen simulations.

3. Results and discussion

3.1. Oxidation, apparent porosity and thermogravimetric tests

Fig. 2 shows the cross-section area of the castable samples after the oxidation tests. The carbon oxidation took place at 600 °C, becoming more intense at higher temperatures. A carbon rich (dark gray or black area) and/or a partially oxidized region (gray area) were observed for the castables attained after thermal treatments at 600, 900 and 1200 °C. Moreover, some distinct regions [(1) white or light gray, (2) gray and (3) dark gray or black] could be identified in the samples fired at 1500 °C. The antioxidant-free (reference material – R) as well as the Al_4SiC_4 containing composition (2A) showed lower oxidation resistance, as larger decarbonized areas were observed (white and gray regions). When compared to the other evaluated refractories, the addition of 2 wt% of B_4C (2B) or the antioxidant blend (Si + BS + B_4C = 5SBC) seemed to be more effective in inhibiting the carbon oxidation as even a non-oxidized core area was detected in the inner part of these samples after firing at 1500 °C (highlighted as number 3 in Fig. 2).

In order to carry out a quantitative evaluation of the oxidation resistance, the decarbonized areas of the castables were measured by using the Image J software. According to the calculated data shown in Fig. 3, the R composition showed the highest oxidation extent (Fig. 3a) as being above 600 °C almost all carbon reacted with $O_{2(g)}$ or $CO_{(g)}$ from the surrounding atmosphere.

Although a darker core region remained in the R and 2A castable samples fired at 1500 °C, its gray color indicated some partial carbon oxidation. Hence, Fig. 3b presents detailed information about the distinct regions identified after firing at the maximum evaluated temperature.

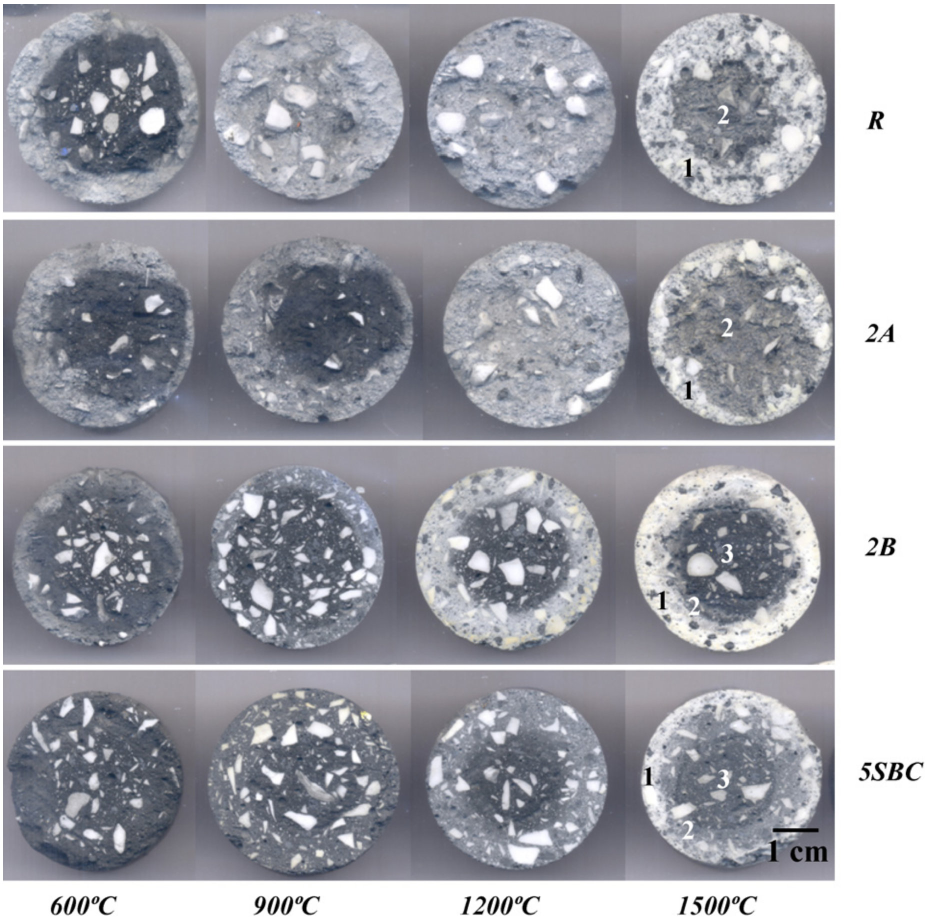

Fig. 2. Oxidation profiles of the evaluated Al_2O_3–SiC–SiO_2–C refractory castables after thermal treatment in oxidizing atmosphere ($pO_2 = 0.21$ atm) (numbers 1, 2 and 3 indicate the totally, partially and non-oxidized areas, respectively).

Based on these results, the Al_4SiC_4 performance was only better than the reference material and, despite the extensive oxidation at high temperatures, a large gray area (partially oxidized) was attained at 1500 °C when 2 wt% of this antioxidant was used. As mentioned above, the addition of 2 wt% of B_4C led to a suitable protection of the carbon particles, resulting in lower total oxidation at 1500 °C (Fig. 3b). Although the sum of the partially and totally oxidized areas are higher for the antioxidant blend-containing castable (5SBC) than the 2B one, an expressive gray region (presenting carbon) could still be detected in this former composition (Fig. 2). Thus, both castables (2B and 5SBC) presented better oxidation resistance performance in the evaluated conditions.

Boron carbide reacts with O_2 and CO at temperatures above 450 °C, resulting in C and B_2O_3 (Eqs. (5) and (6)). These phase transformations are followed by volume increase, inducing

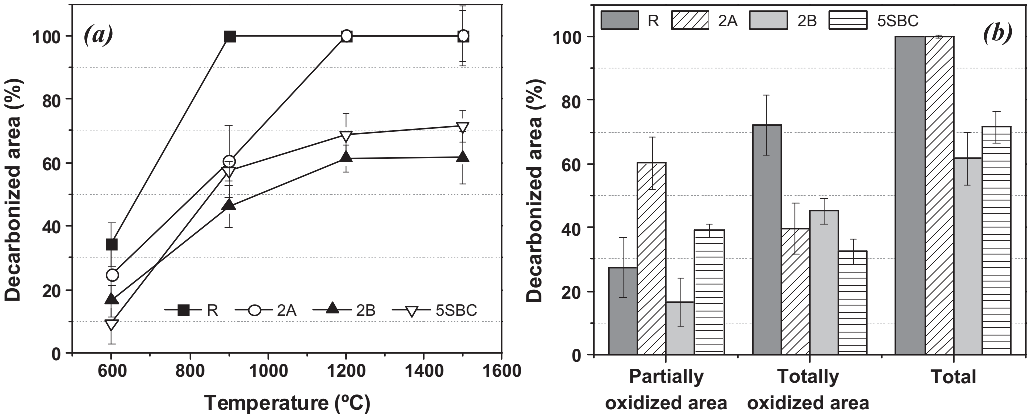

Fig. 3. (a) Calculated decarbonized area of the castable samples as a function of the temperature, based on the gray, light gray and white areas remained. (b) Decarbonized regions of the samples attained after firing at 1500 °C for 5 h in presence of air ($pO_2 = 0.21$ atm).

pore closure [9]. Therefore, the overall outcome is very favorable as the B_4C action not only leads to the carbon protection, but also generates extra C and, due to expansive reactions, the castable porosity can be reduced.

$$B_4C_{(s)} + 3O_{2(g)} \leftrightarrow 2B_2O_{3(l)} + C_{(s)} \qquad (5)$$

$$B_4C_{(s)} + 6CO_{(g)} \leftrightarrow 2B_2O_{3(l)} + 7C_{(s)} \qquad (6)$$

In addition, in the temperature range of 500–800 °C, sodium borosilicate glass (BS) can also form a glassy layer on the surface of the castables also reducing its porosity [8]. As presented in Fig. 4a, a significant porosity decrease in the 2B and 5SBC samples was observed in the evaluated conditions, which helps to explain the lower oxidation of these castables.

The poor performance of the Al_4SiC_4 additive could also be related to the formation of small cracks on the fired samples surfaces (Fig. 4b), affecting the porosity results and increasing the deterioration process due to the greater oxygen infiltration in the refractory structure. In order to understand these effects, thermogravimetric tests of the carbon sources, Al_4SiC_4 and a mixture of Al_4SiC_4 + pitch were carried out and the results are shown in Fig. 5.

Regarding the reactivity of the used carbon sources, pitch, carbon black (amorphous) and coke (partially crystallized) started oxidizing at approximately 400, 450 and 600 °C, respectively (Fig. 5a). Carbon from pitch can be graphitized at elevated temperatures and the final carbon yield is usually determined by the amount of volatile species that are generated and the initial C content [29]. Pitch is the main carbon source added to the castable samples (5 wt%) and its pyrolysis directly affects the refractory properties, as new carbon bonds can be formed at the beginning of the first thermal treatment [29].

Conversely, Al_4SiC_4 oxidizes above 750 °C in the presence of air ($pO_2 = 0.21$ atm) giving rise to Al_2O_3 and SiO_2 (Eqs. (1) and (2)), which results in an expressive mass gain up to 1400 °C (Fig. 5b). With the progress of the aluminum silicon carbide oxidation, the amount of these oxide phases gradually increases on the surfaces of the antioxidant particles [15]. Moreover, above 1200 °C, the Al_2O_3 and SiO_2 contained in this layer should react with each other forming mullite (Eq. (3)).

In order to simulate a reducing atmosphere, a mixture of pitch and Al_4SiC_4 were also analyzed, where the oxygen comprising the synthetic air reacted with C to form $CO_{(g)}$ and $CO_{2(g)}$ during the experiment, exposing the antioxidant to these gases. Based on Fig. 5c, pitch oxidation was identified between 400 and 680 °C and this component was completely oxidized, as 50 wt% of the initial mixture corresponds to C. Under reducing conditions, some variations can be noticed in the Al_4SiC_4 behavior and its transformation began at approximately 700 °C (Eqs. (7) and (8), and Fig. 5c). Therefore, this antioxidant can be readily oxidized in the presence of oxygen or $CO_{(g)}$ and, considering the raw materials used in the designed castable compositions, the action of this aluminum silicon carbide seems to be limited, as pitch, carbon black and coke oxidation takes place earlier (Fig. 5a). Despite the Al_4SiC_4 oxidation, it must be highlighted that C generation can take place in a reducing environment (Eqs. (7) and (8)) such as the interior of the 2A castable samples, which could explain the remaining gray area observed in Fig. 2.

$$Al_4SiC_4 + 6CO \rightarrow 2Al_2O_3 + SiC + 9C \qquad (7)$$

$$3Al_2O_3 + 2SiC + 4CO \rightarrow 2Al_6Si_2O_{13} + 6C \qquad (8)$$

As presented in the literature [12,22,23], the Al_4SiC_4 addition in Al_2O_3–C and MgO–C refractory bricks (which have graphite as the main carbon source and much lower porosity when compared to castables) results in better protection, as graphite is usually oxidized above 800 °C. Nevertheless, the attempt to incorporate such crystalline carbon in refractory castables results in additional problems due to its poor wettability in water and flake shape particles which hinders the efficient dispersion and packing of the compositions during the processing step. For this reason, amorphous and partially crystalline carbons are commonly used in castable materials [25].

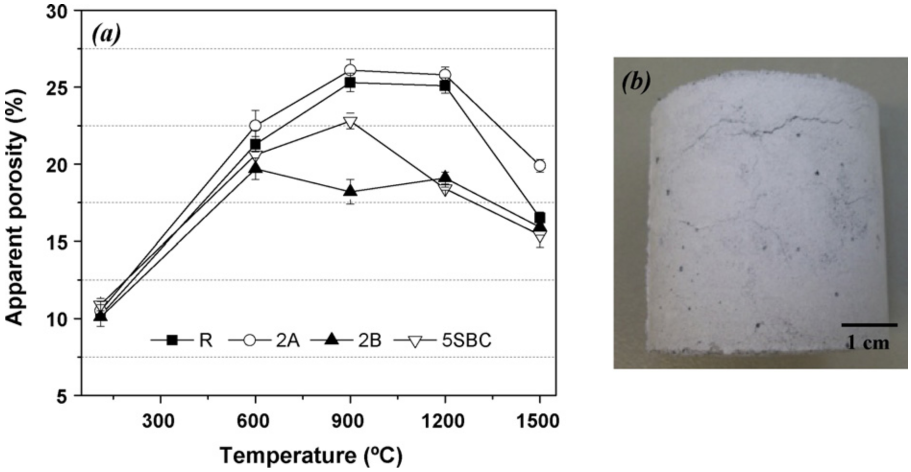

Fig. 4. (a) Apparent porosity of the castable samples after drying at 110 °C and firing at 600, 900, 1200 and 1500 °C in an oxidizing atmosphere. (b) Cracks formed on the Al_4SiC_4 containing samples surface mainly after firing at 900, 1200 and 1500 °C.

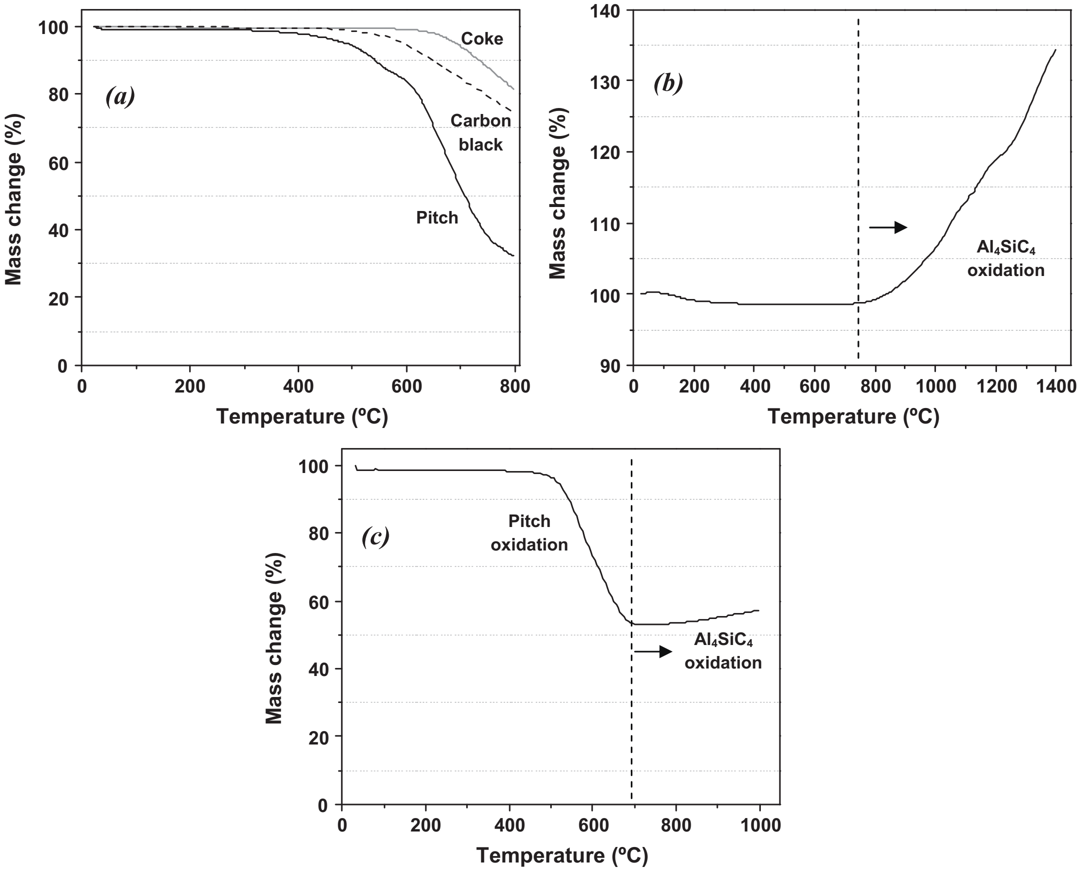

Fig. 5. Mass change of the (a) carbon sources, (b) Al_4SiC_4 and (c) 1:1 wt% mixture of Al_4SiC_4 + pitch as a function of the temperature (heating rate = 5 °C min^{-1}).

According to Fig. 6, the thermodynamic predictions are in tune with the experimental results, as Al_4SiC_4 can readily react with the gaseous phase contained in the atmosphere, forming mainly mullite ($Al_6Si_2O_{13}$), Al_2O_3 and $CO_{(g)}$ or C in the range of 600–1400 °C under the equilibrium condition.

Thus, it can be inferred that the greater carbon oxidation led to the porosity increase in the 2A samples affecting their mechanical strength and inducing the generation of cracks on their surface (Fig. 4). Although the mullite formation is predicted by the thermodynamic calculations to take place at a low temperature (e.g. 600 °C), the kinetic factors play a major role, hindering this reaction below 1100 °C [8,30]. Therefore, the extensive C oxidation should be the main factor responsible for the cracking observed in the samples after firing at 600 and 900 °C.

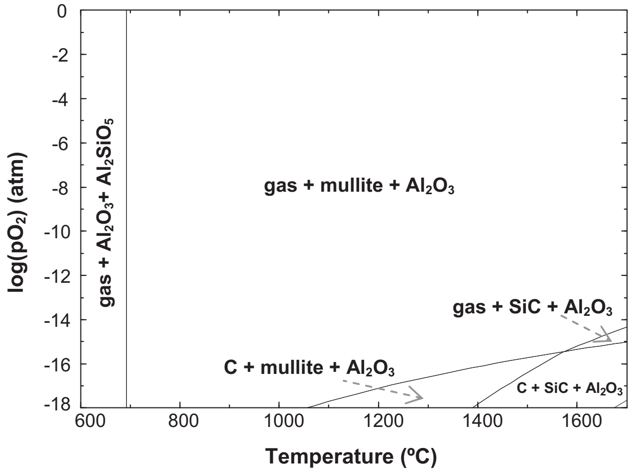

Fig. 6. Phase diagram presenting the Al_4SiC_4 behavior as a function of temperature and oxygen partial pressure.

3.2. Hot elastic modulus, thermodynamic simulations and quantitative XRD analyses

Some transformations (such as densification, crystallization, microcracking, and pore formation) in solid materials are related to changes in the elastic modulus (*E*). Consequently, *E* measurements at high temperatures can be used to evaluate the thermo-mechanical behavior of refractory materials. Fig. 7 presents the *E* results for the R (without antioxidant) and 2A castables collected throughout one thermal cycle up to 1200 °C in oxidizing atmosphere. Hot elastic modulus behavior of the 2B and 5SBC compositions is also presented, but more details and a complete discussion of such results can be found in a previous publication [30].

In general, the elastic modulus profiles presented a hysteresis behavior, which is usual due to crack closures and opening mechanisms that take place during heating and cooling cycles in materials comprising coarse grains [30,31]. Further-

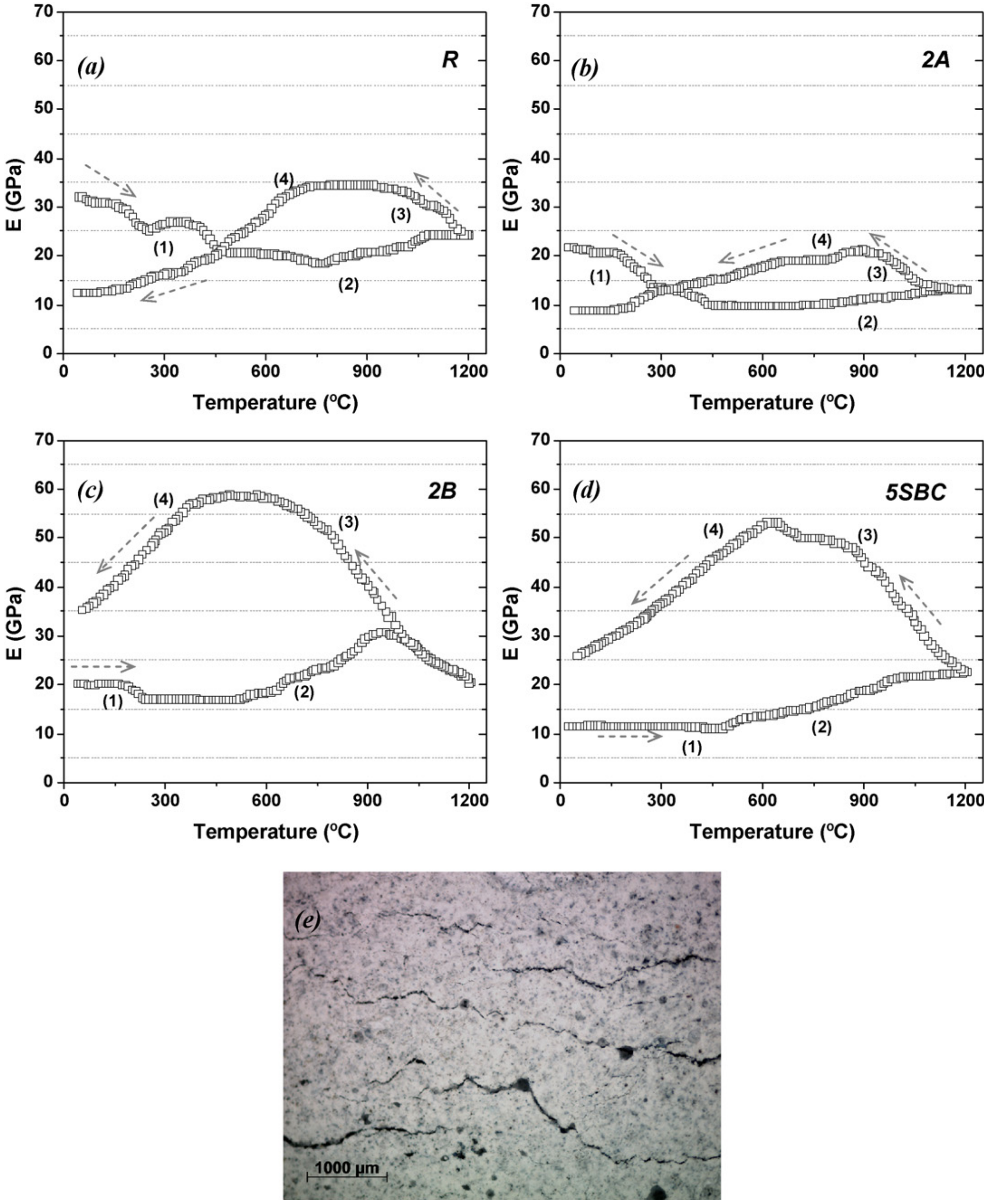

Fig. 7. Elastic modulus evolution as a function of temperature, under oxidizing atmosphere ($pO_2 = 0.21$ atm): (a) R, (b) 2A, (c) 2B and (d) 5SBC samples obtained after curing and drying steps. Numbers 1–4 highlight the main transformations that took place along the first heating and cooling cycle. (e) Surface image of sample 2A attained after the *E* measurements, highlighting the cracks formed.

more, some transformations can be highlighted in order to better explain the *E* changes of the designed castables (Fig. 7):

(1) From 150 up to 450 °C – the initial drop of the R, 2A and 2B curves is associated with the loss of chemically bonded water of the cement hydrated phases (mainly C_3AH_6 and AH_3, where C = CaO, A = Al_2O_3, H = H_2O) and the pitch oxidation. It can also be observed that 2A, 2B and 5SBC samples presented initial elastic modulus values lower than the R one, which is related to their lower alumina content as the open porosity after drying were very close (Fig. 4). Moreover, the intense pitch oxidation in the R and 2A castables resulted in the decrease of the *E* values above 400 °C.

(2) From 750 up to 1200 °C – increasing the temperature, carbonization of the semi-coked phase resulting from the carbon sources reactions will have a critical effect on the castable properties between 600 °C and 800 °C [28]. In addition, castables densification, CA and CA_2 crystallization between 900 and 1200 °C [31], and the Al_4SiC_4 action in the 2A composition should affect the elastic properties of the samples, leading to an *E* increase. Although Fig. 4a presents the porosity increase for the R and 2A castables in the range of 600–1200 °C, it must be highlighted that these

results were not attained throughout the in situ *E* test evaluation heating cycle but only after cooling down the samples to room temperature after a 5-h dwell time at the defined temperature. Another important aspect is that the samples were not kept at 1200 °C during the elastic modulus evaluation after reaching this maximum temperature, therefore, the mullite formation should not have affected the results significantly, presented in Fig. 7.

(3) From 1200 down to 900 °C – during the first part of the cooling cycle, a significant increase in the elastic modulus was observed for the studied castables. This *E* variation is related to the usual stiffening of the material when the temperature drops due to the increase in the liquid phase viscosity and the partial crack closure [30,31]. Although the thermodynamic calculations do not confirm the presence of liquid in the R and 2A compositions at 1200 °C, the formation of this phase is predicted for higher temperatures and a total of 13.2 and 12.1 wt% should be attained in the castables' matrix (dp < 200 μm) at 1500 °C, respectively. However, considering that the samples were not in an equilibrium state, it is expected that a small amount of liquid phase could be formed in some specific regions of the evaluated materials at 1200 °C, which influenced the elastic modulus behavior of such castables. On the other hand, the higher *E* increase detected for the 2B and 5SBC compositions (Fig. 7c and d) are directly related to the presence of a liquid phase (Fig. 8) that was mainly comprised by Al_2O_3, CaO, SiO_2 (derived from silica fume and SiC oxidation) and B_2O_3.

(4) From 900 down to 30 °C – the further decay of *E* values is associated with the development of new flaws (i.e., opening of the cracks partially closed during the beginning of the cooling cycle or new crack formation) induced by the thermal expansion mismatch among the phases comprising the castables' samples. Various mechanisms can simultaneously take place in a cooling cycle (micro-displacements between grains within the matrix, interfacial decoherences between phases, microcracking, etc.). Thus, difficulties are found and few sound conclusions can be drawn [30]. Nevertheless, although an expressive decrease in *E* was attained for the reference, 2B and 5SBC compositions, it started only below 600 °C, confirming the higher thermomechanical stability of these castables. On the other hand, 2A samples showed a continuous decrease in the elastic modulus below 900 °C, which could be related to the cracks formed on the refractory surface (Fig. 7b).

Regarding the phases contained in the castables' compositions at high temperatures, the thermodynamic calculations mainly predict the presence of Al_2O_3, Al_2SiO_5, anorthite ($CaAl_2Si_2O_8$), SiO_2, mullite, $Al_{18}B_4O_{33}$ and a liquid phase under oxidizing atmosphere ($pO_2 = 0.21$ atm) (Fig. 8). How-

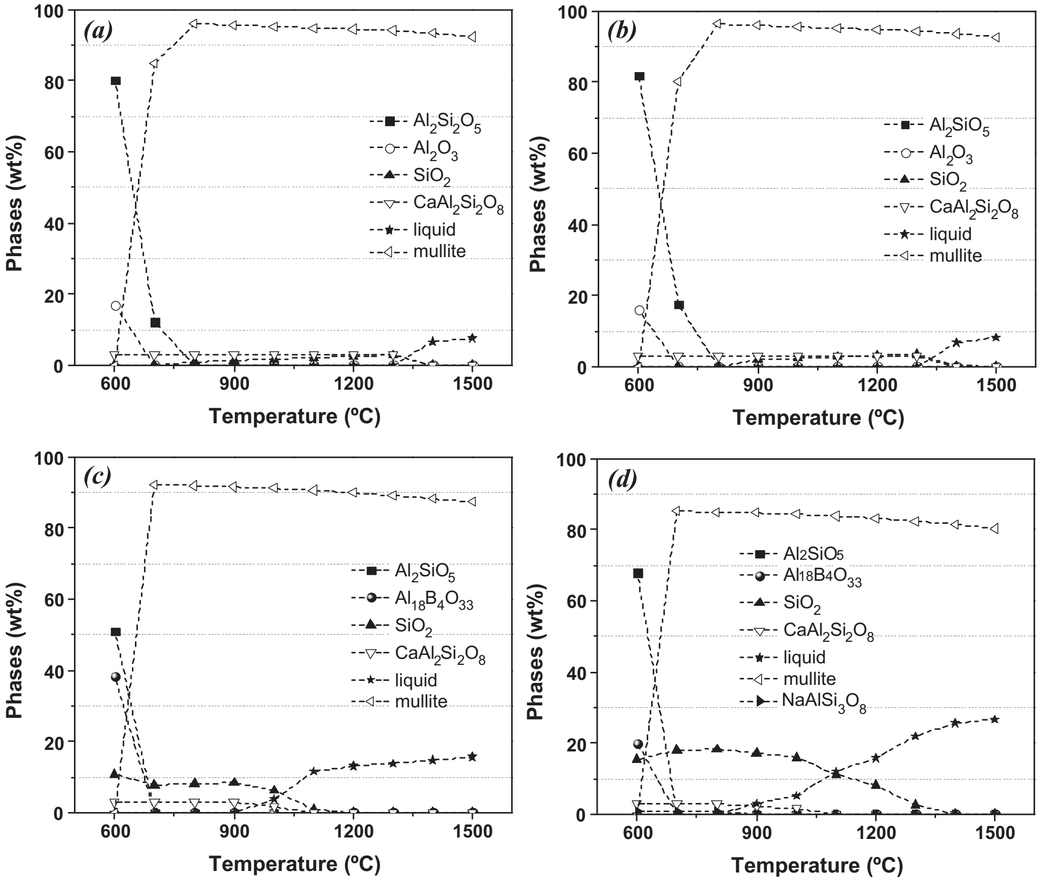

Fig. 8. Thermodynamic predictions of the phases contained in the carbon containing castables (a) R, (b) 2A, (c) 2B and (d) 5SBC, when exposed to an oxidizing atmosphere ($pO_2 = 0.21$ atm) as a function of the temperature.

ever, as observed in Fig. 2, the actual refractory samples were not totally oxidized indicating that they did not reach the equilibrium state and, therefore, some differences between the thermodynamic and quantitative XRD results were expected. Table 2 presents the phases' content (obtained by the Rietveld method) of the designed castables as a function of the firing temperature.

According to these data, carbon and SiC oxidation were still detected for all evaluated samples. Additionally, SiO_2 generation (derived mainly from SiC reaction with $CO_{(g)}$) followed by its reaction with Al_2O_3, led to mullite formation at 1200 °C and 1500 °C. As observed in the thermodynamic analysis (Fig. 8), few changes were identified for the XRD results of the R and 2A castables (Table 2), and the greater $Al_6Si_2O_{13}$ (mullite) content of the latter (at 1500 °C) was the main difference between them. Therefore, the expressive carbon oxidation between 400 and 750 °C (due to the high reactivity of the carbon sources with oxygen, taking place earlier than the Al_4SiC_4 action) should be the main factor responsible for spoiling the 2A castable properties in the evaluated temperature range (600–1500 °C). Furthermore, during the cooling step, the development of cracks most likely occurred due to the thermal expansion mismatch among the phases comprising the samples.

Despite the high content of $Al_6Si_2O_{13}$ in the 2B and 5SBC compositions, the B_4C and BS antioxidants led to the generation of low melting temperature phases (mainly B_2O_3 which further reacted with Al_2O_3, forming $Al_4B_2O_9$ and $Al_{18}B_4O_{33}$ [9]), allowing a better accommodation of the stresses induced, as the mullite formation is followed by a volumetric expansion of ~10.4% [15]. The thermodynamic predictions (Fig. 8) seem to support this statement, as a liquid phase is expected to be formed in the range of 900–1500 °C in these castables. Therefore, no visible long cracks, higher *E* values and lower carbon oxidation were attained for the samples containing B_4C or $Si + B_4C + BS$ antioxidants, indicating that these additives induce a better protection to the carbon sources and inhibit some of the negative effects arising from the thermal expansion mismatch between the phases.

Table 2
Quantitative X-ray results of the fired samples attained after the oxidation tests (average standard deviation was close to ± 1%).

Compositions	Phases (wt%)	Temperature (°C)			
		600	900	1200	1500
R	Corundum	79.3	84.7	87.3	59.1
	C	5.5	1.8	0.8	4.0
	SiC[a]	15.2	13.5	10.9	4.5
	SiO_2	–	–	–	5.2
	$Al_6Si_2O_{13}$	–	–	1.0	27.2
2A	Corundum	82.9	82.8	88.0	55.1
	C	8.2	4.4	0.7	5.0
	SiC[a]	8.9	12.8	10.3	3.2
	SiO_2	–	–	–	1.1
	$Al_6Si_2O_{13}$	–	–	1.0	35.6
2B	Corundum	81.3	65.5	49.5	43.1
	C	7.0	5.0	2.8	6.3
	SiC[a]	11.7	9.6	8.6	5.3
	SiO_2	–	–	1.1	4.2
	$Al_6Si_2O_{13}$	–	–	25.4	35.2
	$Al_4B_2O_9$	–	19.9	–	–
	$Al_{18}B_4O_{33}$	–	–	12.6	5.9
5SBC	Corundum	86.5	76.8	39.9	34.4
	C	7.6	8.2	3.2	7.3
	SiC[a]	10.0	9.8	8.9	5.5
	Si	5.0	5.2	1.1	–
	SiO_2	–	–	21.6	7.8
	$Al_6Si_2O_{13}$	–	–	19.1	41.9
	$Al_4B_2O_9$	–	–	6.2	–
	$Al_{18}B_4O_{33}$	–	–	–	3.1

[a] Polytypes 6H, 33R and 3C.

4. Conclusions

Based on the results, although the aluminum silicon carbide additive is pointed out as a promising antioxidant for refractory bricks, its performance proved to be limited to control the carbon oxidation of the designed Al_2O_3–SiC–SiO_2–C refractory castables. Due to the high reactivity of the used carbon sources (coke, pitch and carbon black) with oxygen just above 400 °C; taking place earlier than the Al_4SiC_4 action (>750 °C); the intense carbon oxidation between 400 and 750 °C coupled with the thermal expansion mismatch among the castable phases during cooling were defined as the main factors responsible for spoiling the 2A refractory properties.

Comparing to the other evaluated compositions, the addition of B_4C or the blend of $Si + B_4C + BS$ was more effective in protecting the carbon particles, and no cracks were found on the samples' surface. Thus, although Al_4SiC_4 antioxidant was considered as a good alternative to carbon-containing refractory bricks (mainly Al_2O_3–C or MgO–C, presenting lower porosity and graphite as the main carbon source), some drawbacks were identified when it was applied to castables. In order to avoid some of the identified problems and improve the performance of the compositions containing such an antioxidant, the combined use of B_4C + Al_4SiC_4 (as their action takes place mainly at 450–750 °C and above 750 °C, respectively) for attaining a better control of the carbon oxidation in a broader temperature range is suggested.

Acknowledgments

The authors are grateful to the Federation for International Refractory Research and Education (FIRE), the Brazilian Research Funding CNPq for supporting this work, and to Magnesita Refratários S. A. (Brazil), Almatis (Brazil), Alcoa Alumínio S/A (Brazil), Kerneos (France), Treibacher (Brazil), Unimetal (Brazil), Nacional Grafite (Brazil) and Elkem Refractories (Brazil) for kindly supplying the raw materials.

References

[1] S. Zhang, W.E. Lee, Carbon containing castables: current status and future prospects, Br. Ceram. Trans. 101 (1) (2002) 1–8.

[2] N. Prompt, E. Ouedraogo, High temperature mechanical characterization of an alumina refractory concrete for Blast Furnace main trough. Part I. General context, J. Eur. Ceram. Soc. 28 (15) (2008) 2859–2865.

[3] E. Ouedraogo, N. Prompt, High temperature mechanical characterization of an alumina refractory concrete for Blast Furnace main trough. Part II. Material behavior, J. Eur. Ceram. Soc. 28 (15) (2008) 2867–2875.

[4] S.K. Sadrnezhaad, Z.A. Nemati, S. Mahshid, S. Hosseini, B. Hashemi, Effect of Al antioxidant on the rate of oxidation of carbon in MgO–C refractory, J. Am. Ceram. Soc. 90 (2) (2007) 509–515.

[5] A.S. Gokce, C. Gurcan, S. Ozgen, S. Aydin, The effect of antioxidants on the oxidation behaviour of magnesia–carbon refractory bricks, Ceram. Int. 34 (2) (2006) 323–330.

[6] S. Zhang, N.J. Marriot, W.E. Lee, Thermochemistry and microstructures of MgO–C refractories containing various antioxidants, J. Eur. Ceram. Soc. 21 (2001) 1037–1047.

[7] S. Hayashi, S. Takanaga, H. Takahashi, A. Watanabe, Behavior of boric compounds added in MgO–C bricks, Taikabutsu Overseas 11 (3) (1991) 12–19.

[8] A.P. Luz, V.G. Domiciano, M.A.M. Brito, V.C. Pandolfelli, Thermomechanical properties and post-mortem evaluation of Al_2O_3–SiO_2–SiC–C refractory castables, J. Tech. Assoc. Refract. Japan 29 (3) (2009) 83–86.

[9] A.P. Luz, F.A.O. Valenzuela, V.G. Domiciano, M.A.M. Brito, V.C. Pandolfelli, Improved oxidation resistance of high-carbon-containing castables via antioxidant blend, Am. Ceram. Soc. Bull. 88 (3) (2009) 40–46.

[10] M. Rigaud, New Additives in Carbon-bonded Refractories. Ceramic: Charting the Future, Techna Srl, 1995,, p. 399.

[11] S. Hanagiri, T. Harada, S. Aso, S. Fujihara, H. Yasui, S. Takanaga, H. Takahashi, A. Watanabe, Effects of the addition of metal and CaB6 to magnesia carbon bricks for converters, Taikabutsu Overseas 13 (3) (1993) 20–27.

[12] S. Zhang, A. Yamaguchi, Effect of Al_4SiC_4 addition to carbon-containing refractories, J. Ceram. Soc. Japan 103 (3) (1995) 235–239.

[13] J. Zhao, W. Lin, A. Yamaguchi, J. Ommyoji, J. Sun, Synthesis of Al_4SiC_4 from alumina, silica and graphite, J. Ceram. Soc. Japan 115 (11) (2007) 761–766.

[14] A.R. Studart, M.D.M. Innocentini, I.R. Oliveira, V.C. Pandolfelli, Reaction of aluminum powder with water in cement-containing refractory castables, J. Eur. Ceram. Soc. 25 (2005) 3135–3143.

[15] A. Yamaguchi, S. Zhang, Synthesis and some properties of Al_4SiC_4, J. Ceram. Soc. Japan 103 (1) (1995) 20–24.

[16] K. Inoue, A. Yamaguchi, Synthesis of Al_4SiC_4, J. Am. Ceram. Soc. 86 (6) (2003) 1028–1030.

[17] X. Huang, G. Wen, Reaction synthesis of aluminum silicon carbide ceramics, Mater. Chem. Phys. 97 (2006) 193–199.

[18] V.J. Barczak, Optical X-ray powder diffraction data for Al_4SiC_4, J. Am. Ceram. Soc. 44 (1961) 299.

[19] O. Yamamoto, M. Ohtani, T. Sasamoto, Preparation and oxidation of Al_4SiC_4, J. Mater. Res. 17 (4) (2002) 774–778.

[20] R. Wills, S. Goodrich, Ceramic Engineering and Science Proceedings, vol. 26, 2005, pp. 181–188.

[21] M. Hasegawa, K. Itatani, M. Aizawa, F.S. Howell, A. Kishioka, Low-temperature synthesis of aluminum silicon carbide using ultrafine aluminum carbide and silicon carbide powders, J. Am. Ceram. Soc. 79 (1996) 275–278.

[22] S. Zhang, A. Yamaguchi, A comparison of Al, Si and Al4SiC4 added to Al_2O_3–C refractories, in: Proceedings of the UNITECR 1997 (2), 1997, pp. 861–868.

[23] L. Li, S.F. Wang, S.B. Chen, The improvement in oxidation resistance of magnesia carbon refractory bricks by Al_4SiC_4, Mater. Sci. Forum 686 (2011) 671–677.

[24] R.G. Pileggi, A.R. Studart, M.D.M. Innocentini, V.C. Pandolfelli, High performance refractory castables, Am. Ceram. Soc. Bull. 81 (2002) 37–42.

[25] I.R. Oliveira, R. Salomão, V.C. Pandolfelli, A.R. Studart, High-carbon-content refractory castables, Am. Ceram. Soc. Bull. 82 (10) (2003) 951–958.

[26] I.R. Oliveira, P. Sepulveda, V.C. Pandolfelli, Deflocculation of Al_2O_3–SiC suspensions, Am. Ceram. Soc. Bull. 80 (2) (2001) 47–53.

[27] R.G. Pileggi, A.E. Paiva, J. Gallo, V.C. Pandolfelli, A novel rheometer for refractory castables, Am. Ceram. Soc. Bull. 79 (1) (2000) 54–58.

[28] G. Pickett, Equations for computing elastic constants from flexural and torsional resonant frequencies of vibration of prisms and cylinders, Proc. Am. Soc. Test. Mater. 45 (1945) 846–865.

[29] B. Rand, B. McEnaney, Carbon binders from polymeric resins and pitch. Part I. Pyrolysis behavior and structure of the carbons, Br. Ceram. Trans. J. 84 (1985) 157–165.

[30] A.P. Luz, M. Huger, V.C. Pandolfelli, Hot elastic modulus of Al_2O_3–SiC–SiO_2–C castables, Ceram. Int. 37 (2011) 2335–2345.

[31] M. Dimitrijevic, M. Posarac, J. Majstorovic, T. Volkov-Husovic, B. Matovic, Behavior of silicon carbide/cordierite composite material after cyclic thermal shock, Ceram. Int. 35 (2009) 1077–1081.